Supporting Information

Curvature-Induced Electronic Tuning of Molecular Catalysts for CO_2 Reduction

Pengfei Tian,[#,[a]] Bo Zhang,[#,[b]] Jiacheng Chen,[[a]] Jing Zhang,[[b]] Libei Huang,[[c]] Ruquan Ye,[[c]] Bo Bao,[[a],*] and Minghui Zhu[[a],*]

[a] School of Chemical Engineering, East China University of Science and Technology, Shanghai 200237, China

[b] Key Laboratory of Energy Thermal Conversion and Control of Ministry of Education, School of Energy and Environment, Southeast University, Nanjing, Jiangsu 210096, China

[c] State Key Laboratory of Marine Pollution, Department of Chemistry, City University of Hong Kong, Hong Kong, China.

# These authors contribute equally

* Corresponding author: bbao@ecust.edu.cn; minghuizhu@ecust.edu.cn

1. Supplementary Methods

Theoretical Calculation Details.

The reaction steps considered for the electrochemical reduction of CO_2 to carbon monoxide are as follows:

$$CO_2 + H^+ + e^- + * \rightarrow COOH* \quad (1)$$

$$COOH* + H^+ + e^- \rightarrow CO* + H_2O \quad (2)$$

$$CO* \rightarrow CO + * \quad (3)$$

where * and M* represents a vacant surface-active site and the species (reactants, intermediates and products) adsorbed on the surface.

The Gibbs free energies were calculated using the following equation:

$$G(\mathrm{T}) = E_{DFT} + ZPE + \int_0^T C_{V,\mathrm{vib}} dT - T \cdot S(\mathrm{T}) \quad (4)$$

where E_{DFT}, ZPE, $C_{V,vib}$, T and $S(T)$ are the total energy from DFT calculation, the zero point energy (ZPE) correction, heat capacity, the reaction temperature (298 K) and entropy, respectively. In this work, we applied the same free energy corrections for the gaseous species as Ref.[1] For the surface species, ZPE, $C_{V,vib}$ and $S(T)$ are calculated using equations (5-7):

$$ZPE = \sum_i^{\#vibs} (\frac{1}{2}) h\upsilon_i \quad (5)$$

$$\int_0^T C_{V,\mathrm{vib}} dT = \sum_i^{\#vibs} \frac{h\upsilon_i}{(\mathrm{e}^{\frac{h\upsilon_i}{k_B T}} - 1)} \quad (6)$$

$$S(\mathrm{T}) = k_B \sum_i^{\#vibs} [\frac{h\upsilon_i}{k_B T(\mathrm{e}^{\frac{h\upsilon_i}{k_B T}} - 1)} - \ln(1 - \mathrm{e}^{\frac{-h\upsilon_i}{k_B T}})] \quad (7)$$

2. Supplementary figures

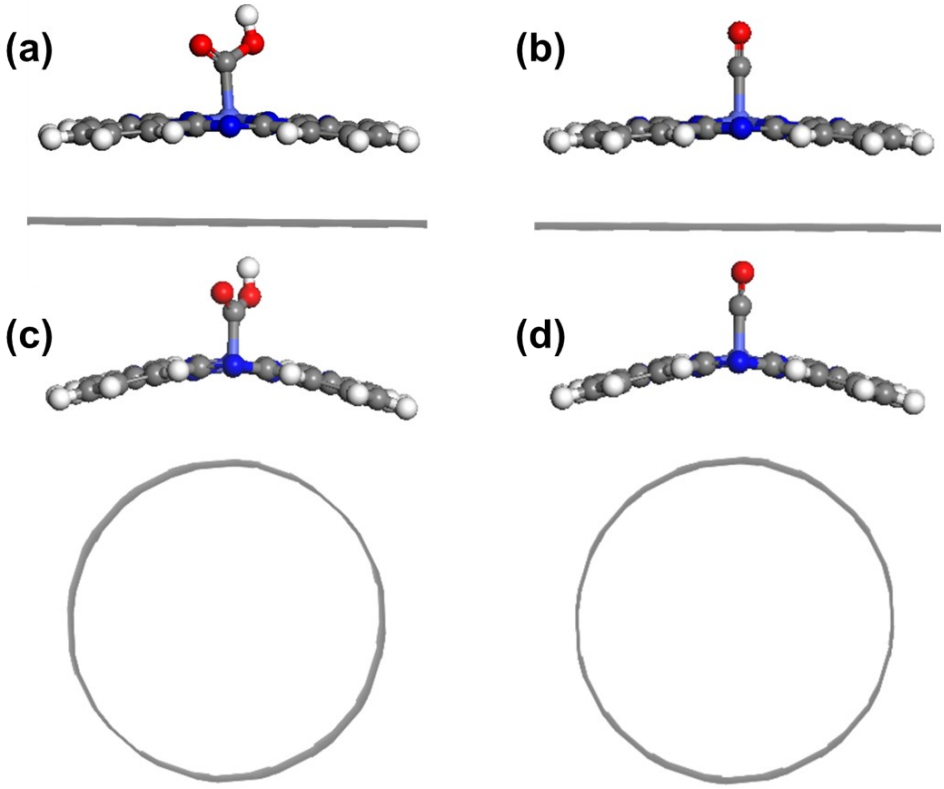

Figure S1. Optimized structures for CoPc-rGO with adsorbed (a) *COOH and (b) *CO intermediates as well as CoPc-CNT with adsorbed (c) *COOH and (d) *CO intermediates.

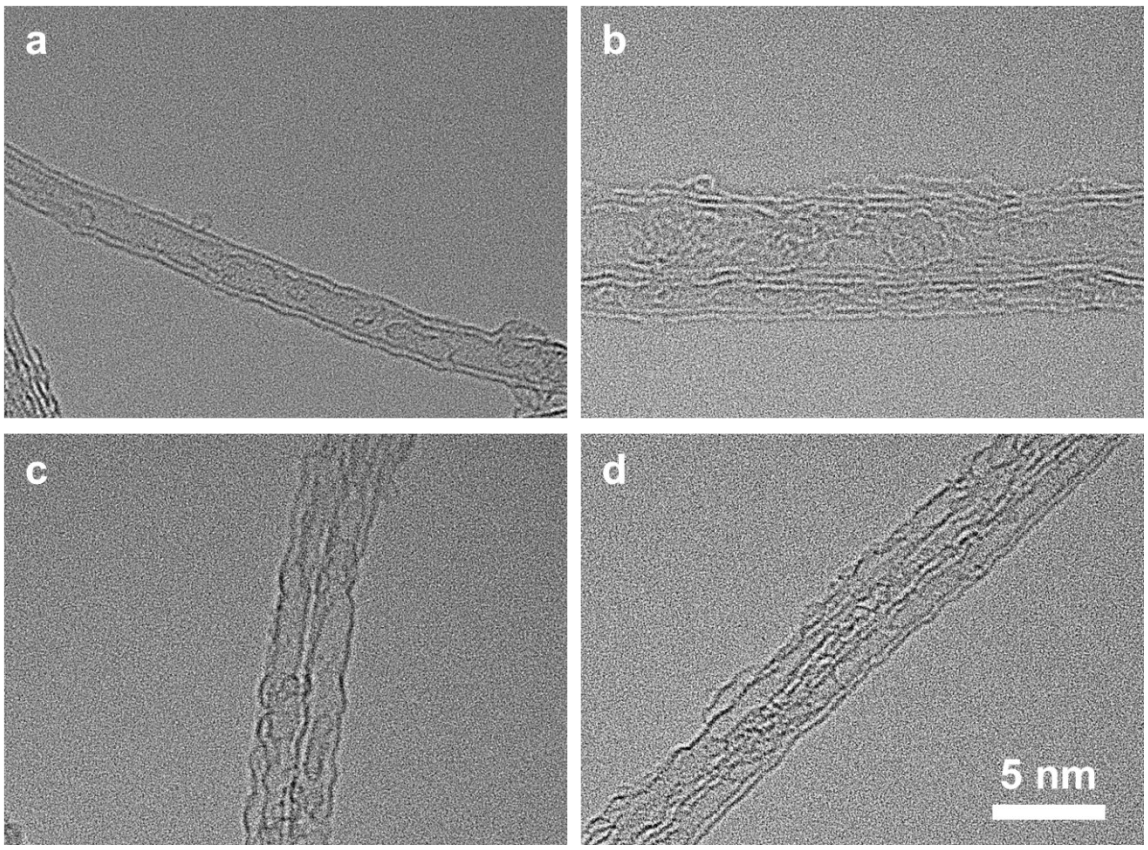

Figure S2. HR-TEM images of CoPc-CNT-1 (Co content: 1.6 wt.%) showing uniform coverage of CoPc with negligible inter-molecular stacking

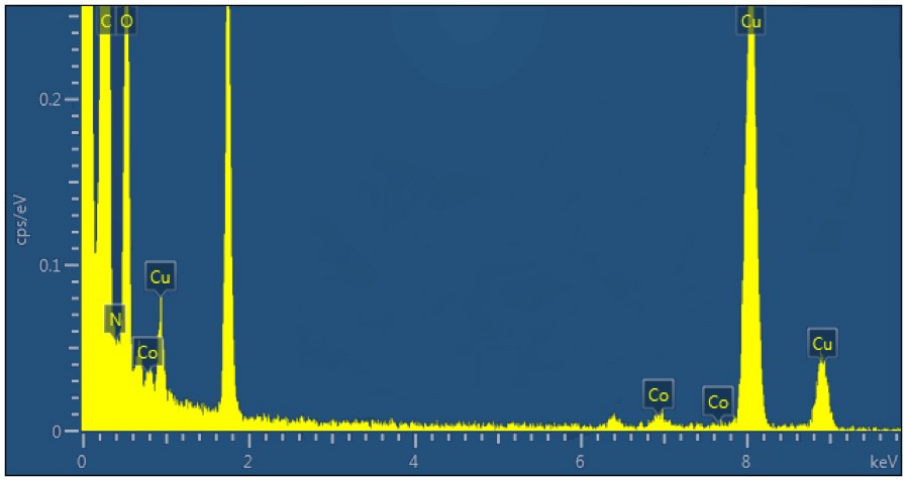

Figure S3. Energy-dispersive x-ray spectroscopy of CoPc-CNT-2 showing the existence of Co, N and C elements.

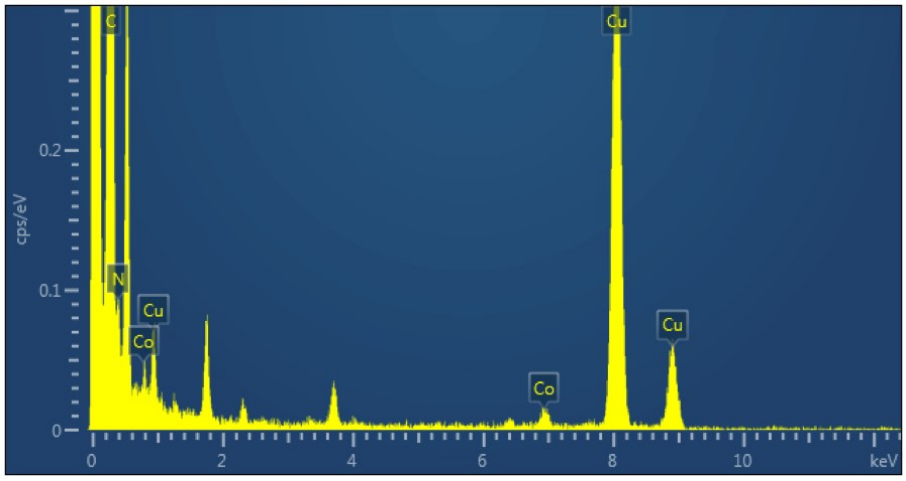

Figure S4. Energy-dispersive x-ray spectroscopy of CoPc-CNT-3 showing the existence of Co, N and C elements.

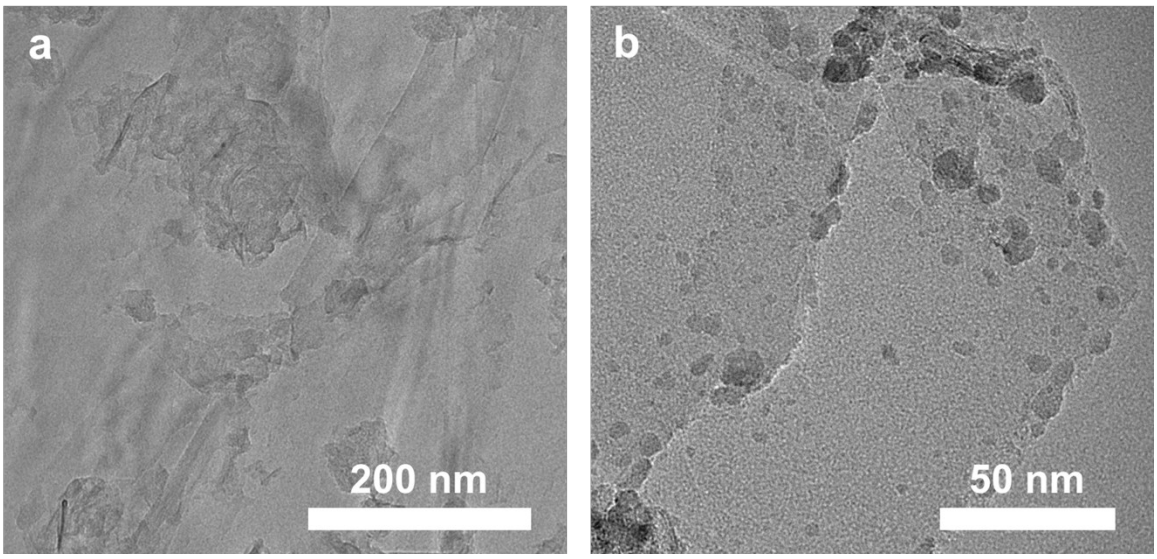

Figure S5. TEM images of (a) CoPc-rGO-1 showing no aggregation and (b) CoPc-rGO-2 showing aggregated CoPc species.

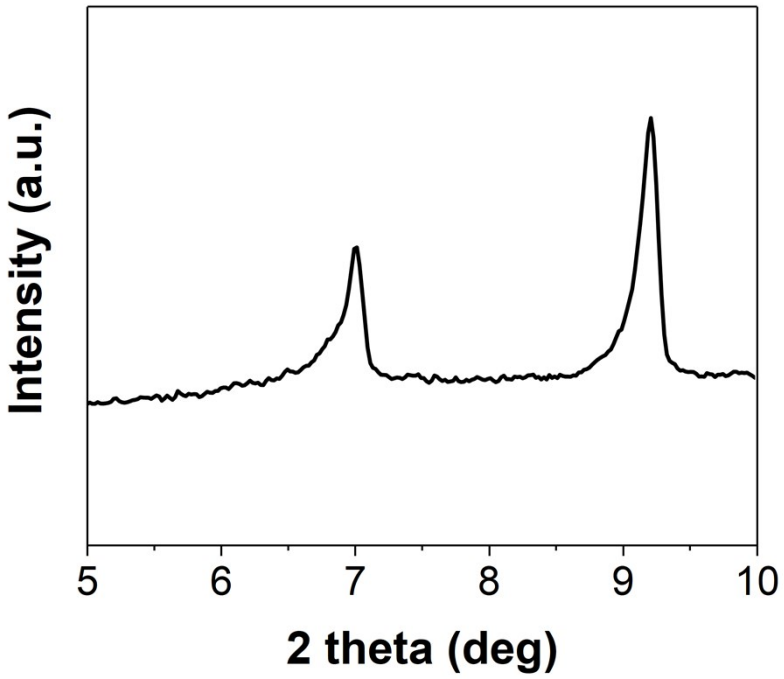

Figure S6. Small angle XRD pattern of CoPc.

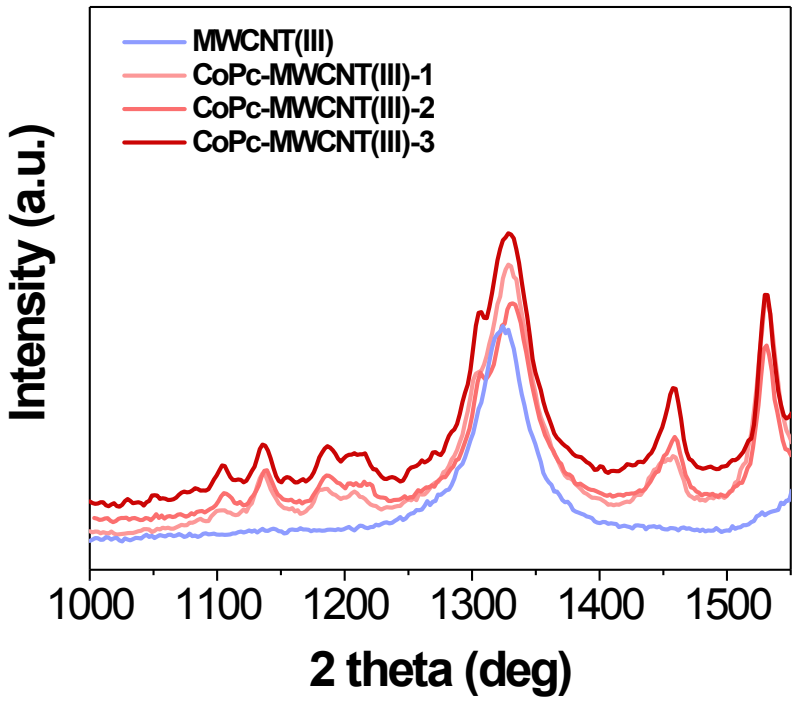

Figure S7. Raman spectrum of CoPc-MWCNT(III) catalysts with various Co loadings.

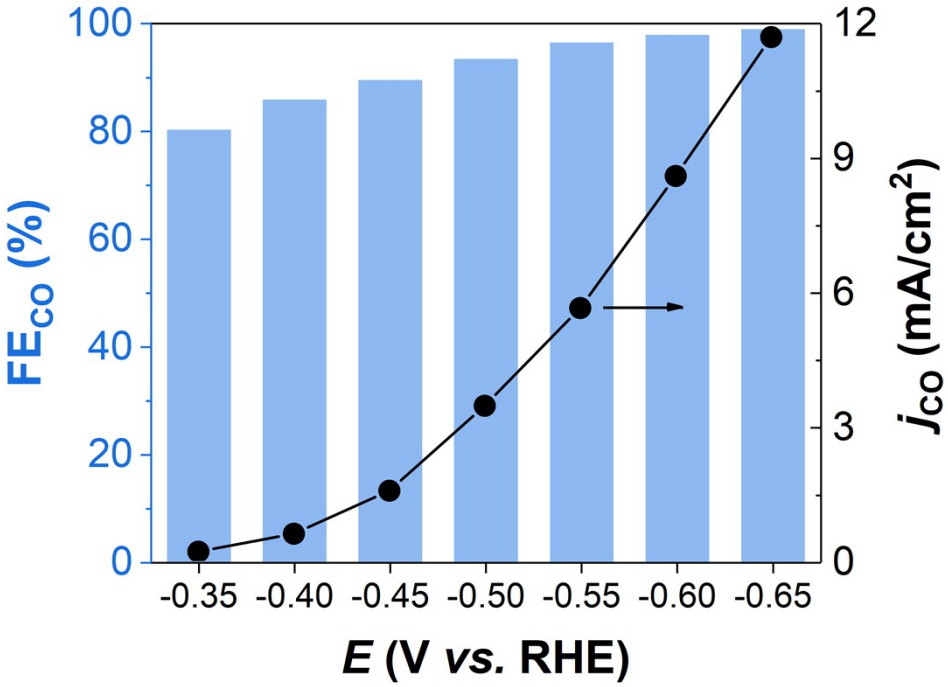

Figure S8. Partial current density and Faradaic efficiency of CO over CoPc-CNT-2 catalyst at various potentials.

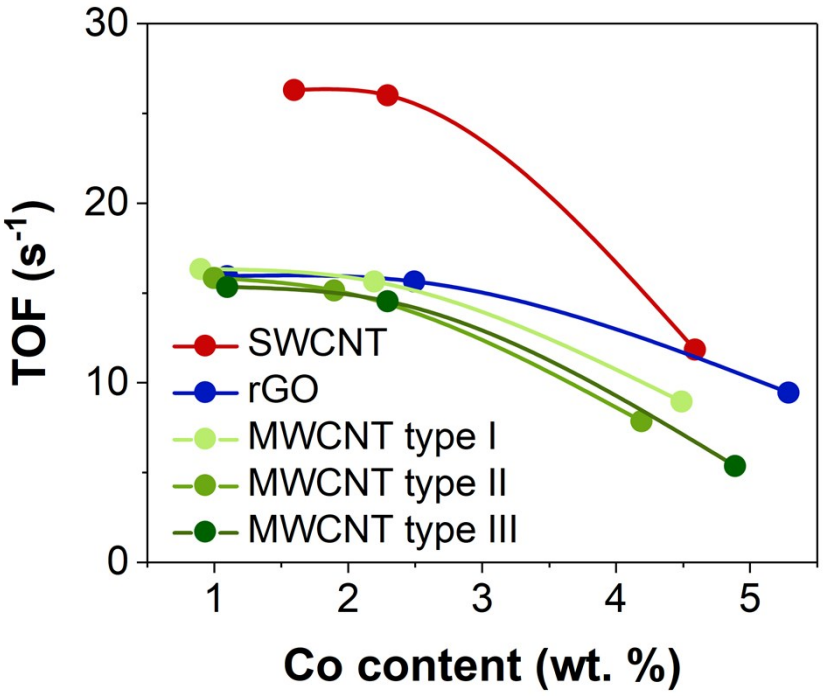

Figure S9. A comparison of TOF_{CO} over CoPc-rGO, CoPc-SWCNT and CoPc-MWCNT catalysts with various Co content at -0.6 V *vs.* RHE

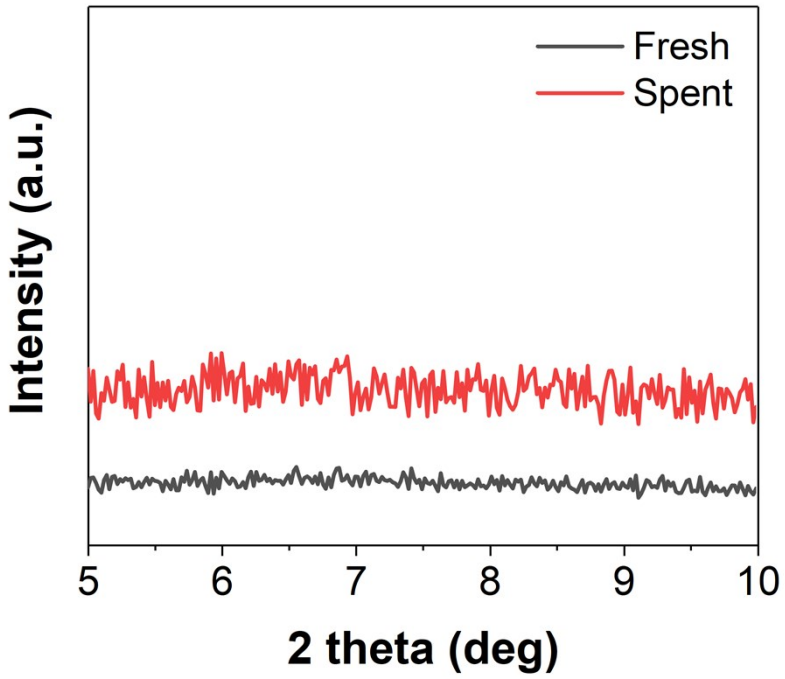

Figure S10. Small angle XRD patterns of fresh CoPc-CNT-2 and the spent catalyst after 12-hour long-term stability test.

3. Supplementary tables

Table S1. Synthesis conditions for supported CoPc catalysts and the corresponding Co content determined by ICP analysis.

Name	**Raw materials for synthesis (mg)**			**Co content by ICP analysis**
	CoPc	Support		
CoPc-rGO-1	10	rGO	100	1.1%
CoPc-rGO-2	25			2.5%
CoPc-rGO-3	100			5.3%
CoPc-CNT-1	10	SWCNT		1.6%
CoPc-CNT-2	25			2.3%
CoPc-CNT-3	100			4.6%
CoPc-MWCNT(I)-1	10	MWCNT(I)		0.9%
CoPc-MWCNT(I)-2	25			2.2%
CoPc-MWCNT(I)-3	100			4.5%
CoPc-MWCNT(II)-1	10	MWCNT(II)		1.0%
CoPc-MWCNT(II)-2	25			1.9%
CoPc-MWCNT(II)-3	100			4.2%
CoPc-MWCNT(II)-1	10	MWCNT(III)		1.1%
CoPc-MWCNT(II)-2	25			2.3%
CoPc-MWCNT(II)-3	100			4.9%

Table S2. Detailed current densities, Faradaic efficiencies and TOF_{CO} for CoPc-CNT at various loadings at -0.6 V *vs.* RHE in 0.75 M $NaHCO_3$ electrolyte.

Catalyst	*j* (mA/cm^2)	FE (%)		TOF_{CO} (s^{-1})
		CO	H_2	
CoPc-CNT-1	6.2	98.3	1.5	26.3
CoPc-CNT-2	8.8	97.8	1.6	26.0
CoPc-CNT-3	8.0	97.8	2.0	11.8

Table S3. Detailed current densities, Faradaic efficiencies and TOF_{CO} for CoPc-rGO at various loadings at -0.6 V *vs.* RHE in 0.75 M $NaHCO_3$ electrolyte.

Catalyst	*j* (mA/cm^2)	FE (%)		TOF_{CO} (s^{-1})
		CO	H_2	
CoPc-rGO-1	2.7	93.4	4.3	15.9
CoPc-rGO-2	6.1	92.0	3.2	15.6
CoPc-rGO-3	7.5	95.5	3.6	9.4

Table S4. A comparison of reported molecular catalysts for the electroreduction of CO_2 to CO in aqueous media to supported CoPc in this work.

Catalyst	*j* (mA/cm^2)	V *vs.* RHE	Electrolyte	FE_{CO}(%)	TOF_{CO}(s^{-1})	Ref.
CoPc-CNT-2	-8.8	-0.60	0.75M $NaHCO_3$	97.8	26.0	This work
CoTPP/CNT	NR	-0.70	0.5M $KHCO_3$	~70	2.75	2
CoPc/CNT	~10.0	-0.63	0.1M $KHCO_3$	92	2.7	3
CoPc-CN/CNT	~15.0	-0.63	0.1M $KHCO_3$	98	4.1	3
CoPc-CN/CNT	~5.6	-0.46	0.5M $KHCO_3$	88	1.4	3
CoPc-P4VP	2.0	-0.73	0.1 M NaH_2PO_4	89	4.8	4
CoPc(py)-P2VP	1.9	-0.73	0.1 M NaH_2PO_4	83	4.2	4
CoPc-F	~6	-0.90	0.5M $KHCO_3$	88	2.05	5
CATpyr/CNT	0.24	-0.59	0.5M $KHCO_3$	93	0.04	6
Co(ch)/CNT	N.A.	-0.83	5.0mM Na_2SO4	89	0.04	7
$Al_2(OH)_2TCPP$-Co	~1	-0.67	0.5M $KHCO_3$	76	0.06	8
COF-367-Co	3.3	-0.67	0.5M $KHCO_3$ (7.3)	91	0.53	9
COF-367-Co(1%)	0.45	-0.67	0.5M $KHCO_3$ (7.3)	53	2.6	9

N.A. means not available.

4. References

(1) Luo, W.; Xie, W.; Mutschler, R.; Oveisi, E.; De Gregorio, G. L.; Buonsanti, R.; Züttel, A. *ACS Catal.* **2018**, *8*, 6571.

(2) Hu, X.-M.; Rønne, M. H.; Pedersen, S. U.; Skrydstrup, T.; Daasbjerg, K. *Angew. Chem. Int. Ed.* **2017**, *56*, 6468.

(3) Zhang, X.; Wu, Z.; Zhang, X.; Li, L.; Li, Y.; Xu, H.; Li, X.; Yu, X.; Zhang, Z.; Liang, Y.; Wang, H. *Nat. Commun.* **2017**, *8*, 14675.

(4) Kramer, W. W.; McCrory, C. C. L. *Chem. Sci.* **2016**, *7*, 2506.

(5) Morlanés, N.; Takanabe, K.; Rodionov, V. *ACS Catal.* **2016**, *6*, 3092.

(6) Maurin, A.; Robert, M. *J. Am. Chem. Soc.* **2016**, *138*, 2492.

(7) Aoi, S.; Mase, K.; Ohkubo, K.; Fukuzumi, S. *Chem. Commun.* **2015**, *51*, 10226.

(8) Kornienko, N.; Zhao, Y.; Kley, C. S.; Zhu, C.; Kim, D.; Lin, S.; Chang, C. J.; Yaghi, O. M.; Yang, P. *J. Am. Chem. Soc.* **2015**, *137*, 14129.

(9) Lin, S.; Diercks, C. S.; Zhang, Y.-B.; Kornienko, N.; Nichols, E. M.; Zhao, Y.; Paris, A. R.; Kim, D.; Yang, P.; Yaghi, O. M.; Chang, C. J. *Science* **2015**, *349*, 1208.